Supporting Information
for
A Mucin-Deficient Ocular Surface Mimetic Platform for Interrogating Drug Effects on Biolubrication, Anti-Adhesion Properties, and Barrier Functionality

Amy C. Madl,[1,*] Chunzi Liu,[1,*] Daniel Cirera-Salinas,[2]
Gerald G. Fuller,[1] and David Myung[1,3,#]

[1]*Department of Chemical Engineering, Stanford University, Stanford, CA 94305*
[2]*Biologics Analytical Research and Development, Novartis Pharma, Basel, AG 4002, Switzerland*
[3]*Byers Eye Institute, Stanford University School of Medicine, Palo Alto, CA 94303*
* These authors contributed equally to this work
[#] Corresponding Author: David Myung (david.myung@stanford.edu)

Supporting Information

Supplemental Experimental Procedures

1. Glycocalyx Immunofluorescence

Cells were seeded in growth medium on 8-well glass bottom chamber slides treated with bovine collagen coating solution (Cell Applications Inc. 12550) at 37 °C and 5% CO_2 until they reached 100% confluence. After the cells reached confluency, the growth medium was replaced by stratification medium composed of DMEM/F12 supplemented with 10% fetal bovine serum (Gibco™ 26140079), 1% penicillin-streptomycin, and 10 ng/mL EGF recombinant human protein (Gibco™ PHG0311L) to induce differentiation and stratification. For immunofluorescence imaging, samples were treated with the primary antibody mouse anti-MUC1 (1:500, Sigma-Aldrich 05-652) in CO_2 independent stratification medium composed of CO_2 Independent Medium (Gibco™ 18045088) supplemented with 1% penicillin-streptomycin, 1x GlutaMAX, 10% fetal bovine serum, and 10 ng/mL EGF for 2 h at 4 °C. The samples were washed three times with Dulbecco's Phosphate-Buffered Saline containing calcium, magnesium, and glucose (DPBS-G) and then stained with goat anti-mouse AF546 (1:500, Life Technologies) in CO_2 independent stratification medium in the dark for 45 min at 4 °C. Hoechst (1:1000, Invitrogen™), CellMask™ Deep Red (1:1000, Invitrogen™ C10046), and fluorescein-labeled Jacalin (1:1000, Vector Laboratories FL-1151) were also included to stain the nucleus, plasma membrane, and O-glycosidically linked oligosaccharides, respectively. Samples were washed three times with DPBS-G and fixed with 4% (w/v) paraformaldehyde in DPBS-G for 15 min at room temperature. Samples were then washed three times with DPBS-G and imaged using a Nikon LSM780 confocal microscope. Images were analyzed using ImageJ software (NIH).

2. Dynamic Light Scattering

Dynamic light scattering was performed on a Brookhaven Instrument Nanobrook Omni.

Supplemental Figures and Tables

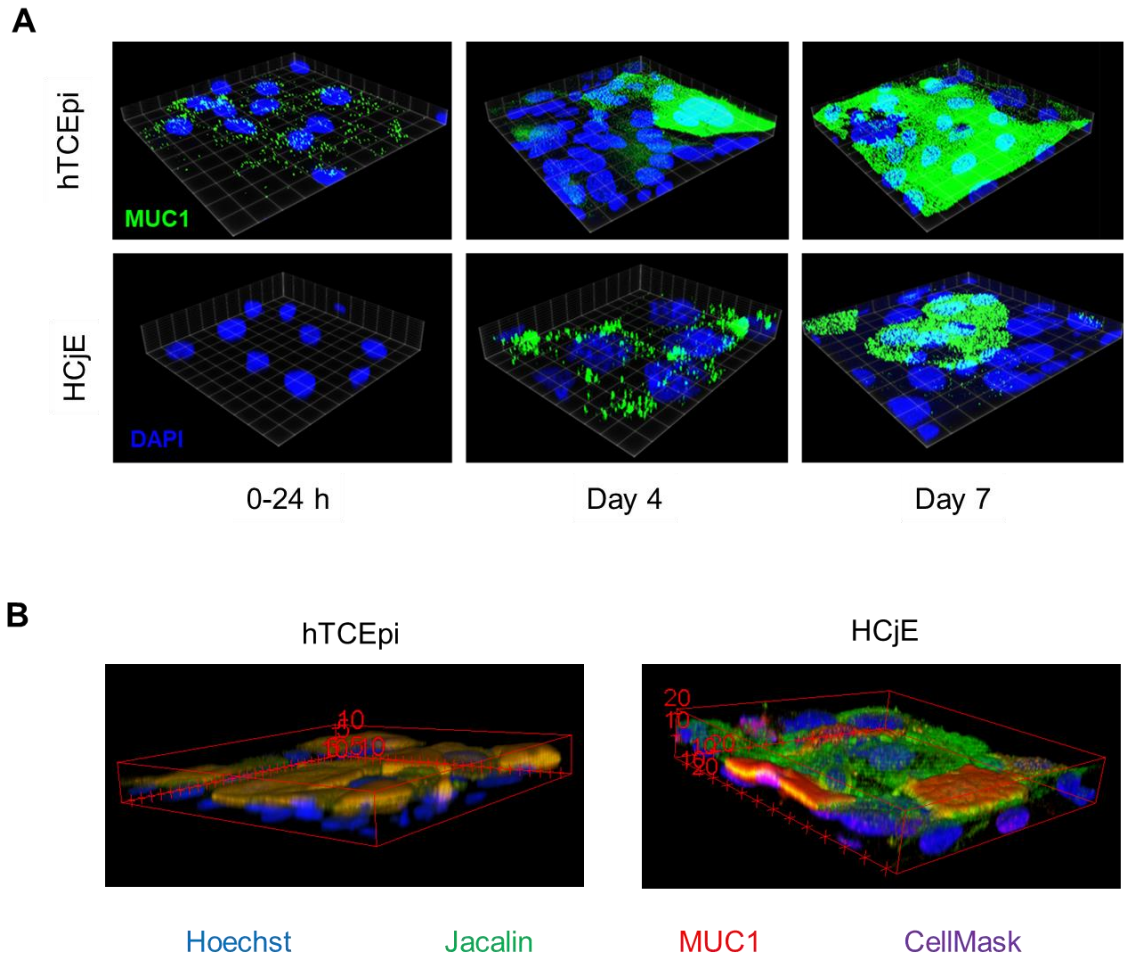

Figure S1. Differentiated hTCEpi and HCjE cells exhibited physiological mucin expression and hierarchical architecture. **(A)** hTCEpi and HCjE cells stratified and began to express the membrane-associated mucin MUC1 over 7 days in culture in stratification medium. **(B)** After 5 days in stratification medium, a reasonably homogenous glycocalyx began to form on the apical surfaces of both HCjE and hTCEpi cells, as visualized by O-glycan staining with Jacalin and immunofluorescence staining for MUC1.

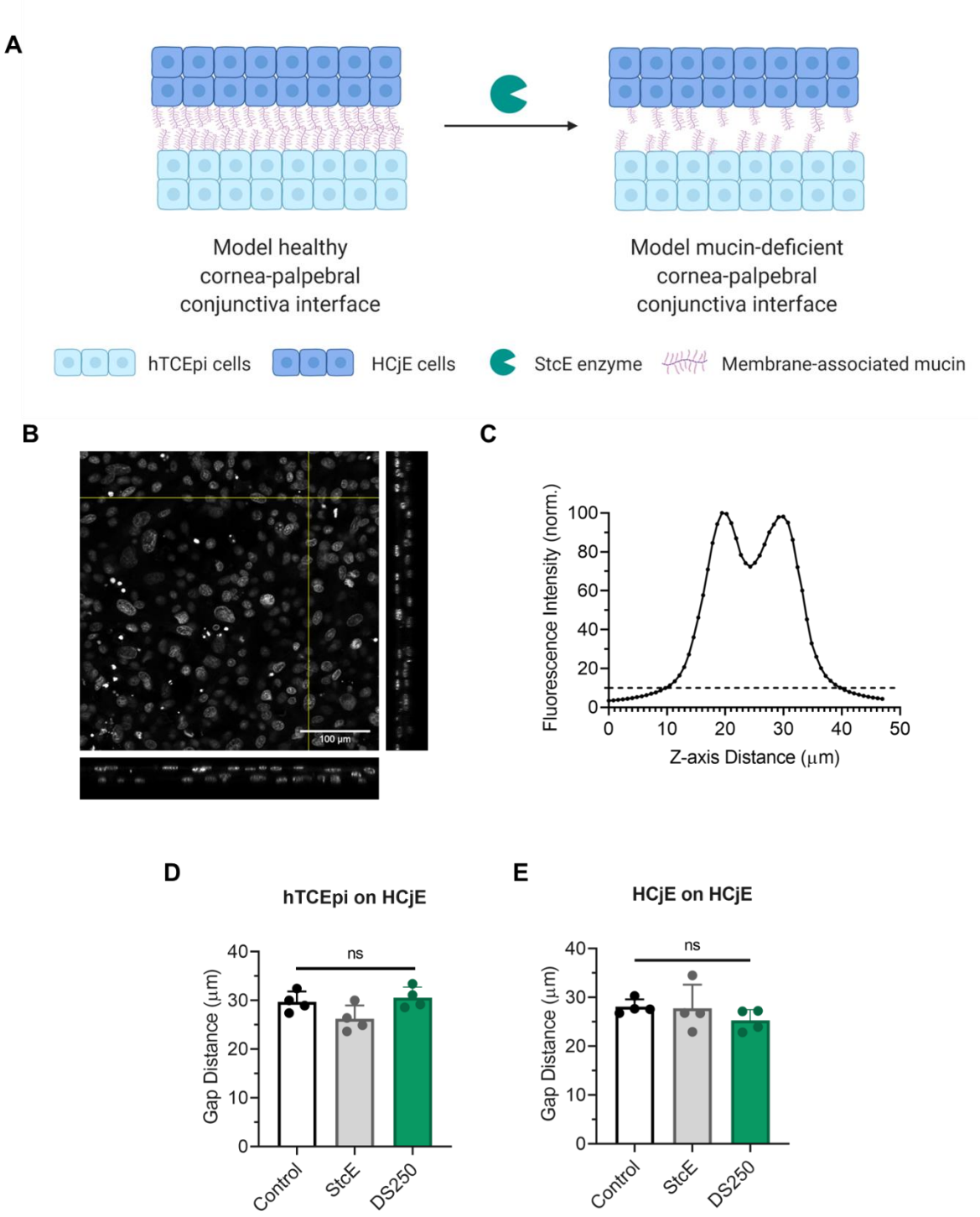

Figure S2. Induced mucin deficiency did not significantly alter gap distance or the mechanical properties of ocular cells. **(A)** Idealized schematic depicting model healthy and mucin-deficient cornea-palpebral conjunctiva interfaces used in the DED LCR model. Created with BioRender.com. **(B)** Representative orthogonal projections of Hoechst-labeled differentiated

HCjE cells in contact with Hoechst-labeled differentiated HCjE cells (scale bar: 100 μm). **(C)** Representative z-axis profile of normalized fluorescence intensity for Hoechst-labeled differentiated hTCEpi cells in contact with Hoechst-labeled differentiated HCjE cells. **(D, E)** StcE treatment and StcE treatment followed by supplementation with 250 μg/mL recombinant human lubricin (DS250) did not significantly affect the gap distance for Hoechst-labeled differentiated HCjE cells in contact with Hoechst-labeled differentiated **(D)** hTCEpi or **(E)** HCjE cells, respectively (data = mean ± S.D., n = 4). Statistical significance ($p < 0.05$) was determined using one-way Welch ANOVA with post-hoc Dunnett's T3 multiple comparisons testing. Statistical significance ($p < 0.05$) was determined using a two-tailed Welch's t-test.

Variant	Sum of aggregates (> LOQ) (%)	Sum of fragments (> LOQ) (%)	Main (%)
Drug Substance	1.16	0.00	97.3
Temperature Stressed	4.01	11.43	84.6
Acid Stressed	0.00	74.80	24.9
Alkaline Stressed	20.12	8.45	70.1

Table S1. Composition of recombinant human lubricin samples subjected to different temperature and pH conditions.

Variant	Stock	25 µg/mL	75 µg/mL	250 µg/mL
Drug substance	7.0	7.4	7.4	7.4
Temperature stressed	7.0	7.4	7.1 – 7.4	7.1 – 7.4
Acid stressed	4.0	7.4	7.1 – 7.4	7.1
Alkaline stressed	8.0	7.4	7.4	7.4

Table S2. pH values for recombinant human lubricin stock samples and cell culture medium containing different amounts of lubricin.

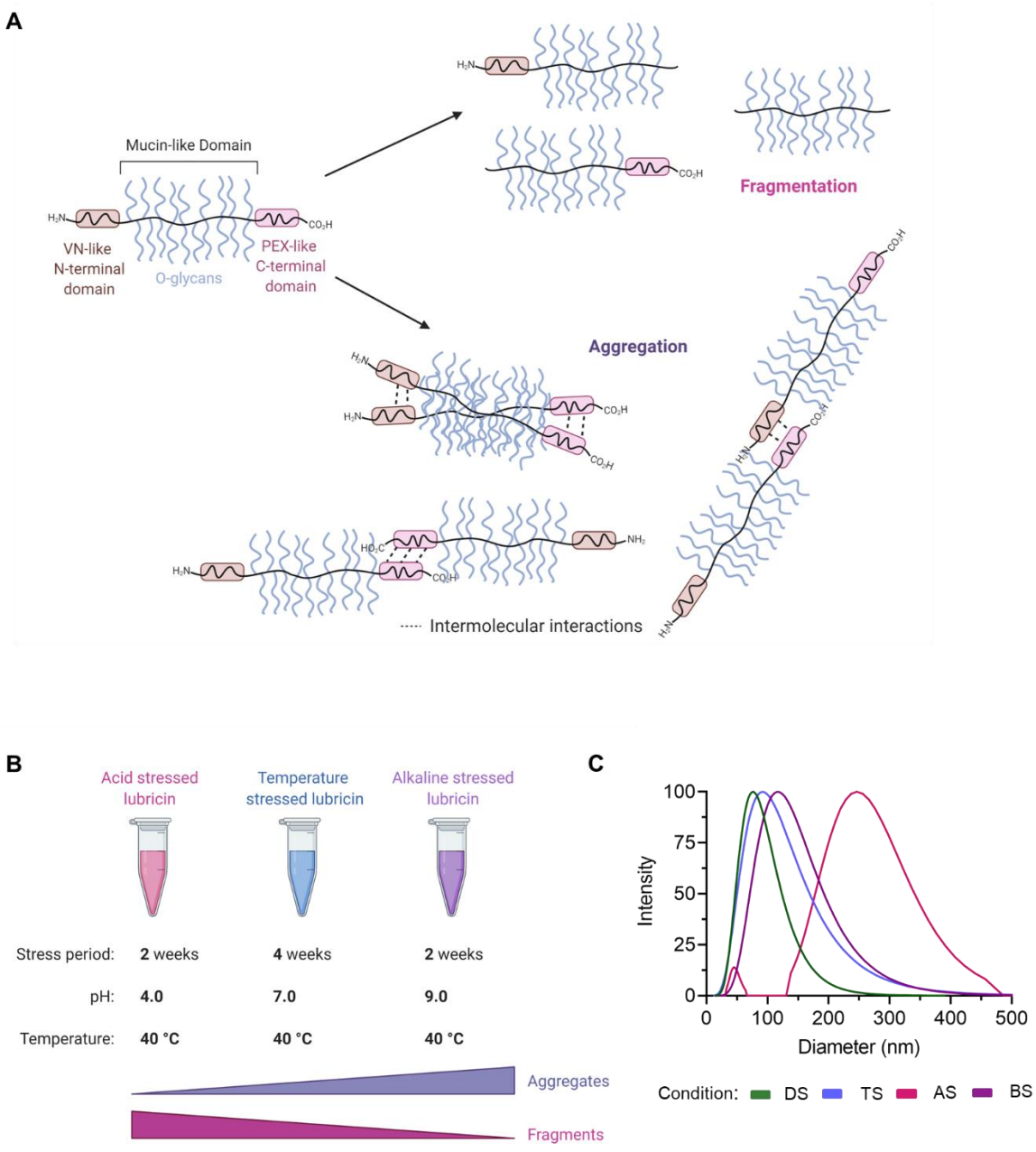

Figure S3. Recombinant human lubricin aggregates and fragments when subjected to accelerated aging conditions. **(A)** Lubricin changed conformation following exposure to high temperature (40 °C) and/or acidic (pH 4.0) or alkaline (pH 9.0) pH conditions. Created with BioRender.com. **(B)** Subjecting lubricin molecules to specific heat and pH conditions produced different mixtures of fragments and aggregates. Created with BioRender.com. **(C)** Dynamic light scattering traces for unstressed recombinant human lubricin (DS) and recombinant human lubricin subjected to temperature stress (TS), acid stress (AS), and alkaline stress (BS).

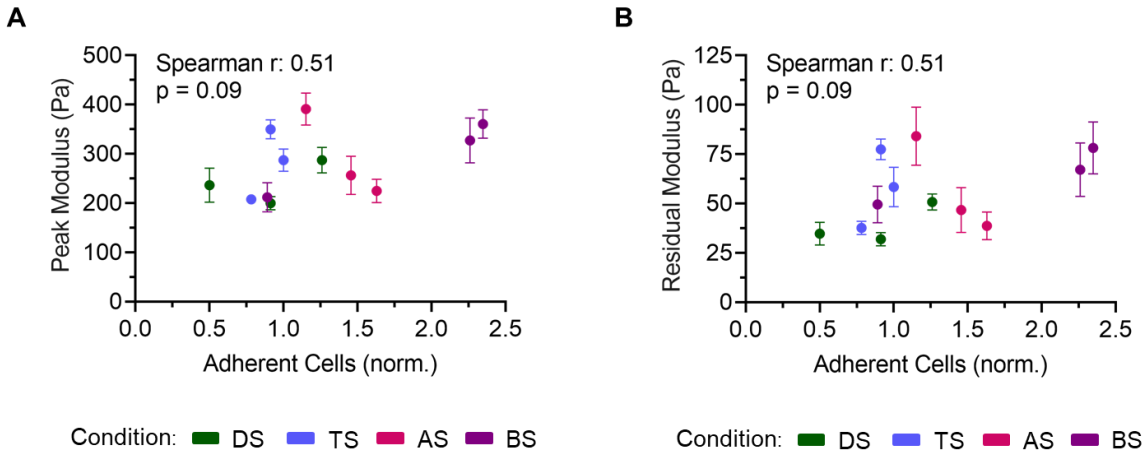

Figure S4. Unstressed and aged lubricin exerts weakly correlated anti-adhesion and biolubrication activity. **(A)** Biaxial plot of normalized adherent cell counts and peak modulus values (data = mean ± S.E., n = 7-12). **(B)** Biaxial plot of normalized adherent cell counts and residual modulus values (data = mean ± S.E., n = 7-12).

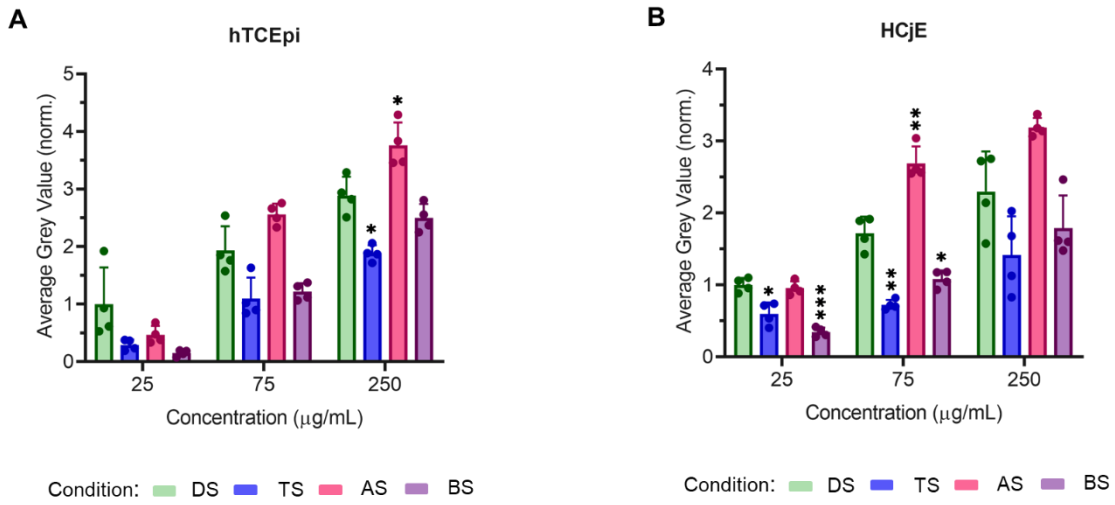

Figure S5. Lubricin displayed similar dose-dependent adsorption behavior on StcE-treated differentiated **(A)** hTCEpi and **(B)** HCjE cells. Statistical significance ($p < 0.05$) was determined within a concentration using one-way Welch ANOVA with post-hoc Dunnett's T3 multiple comparisons testing relative to lubricin drug substance (DS).

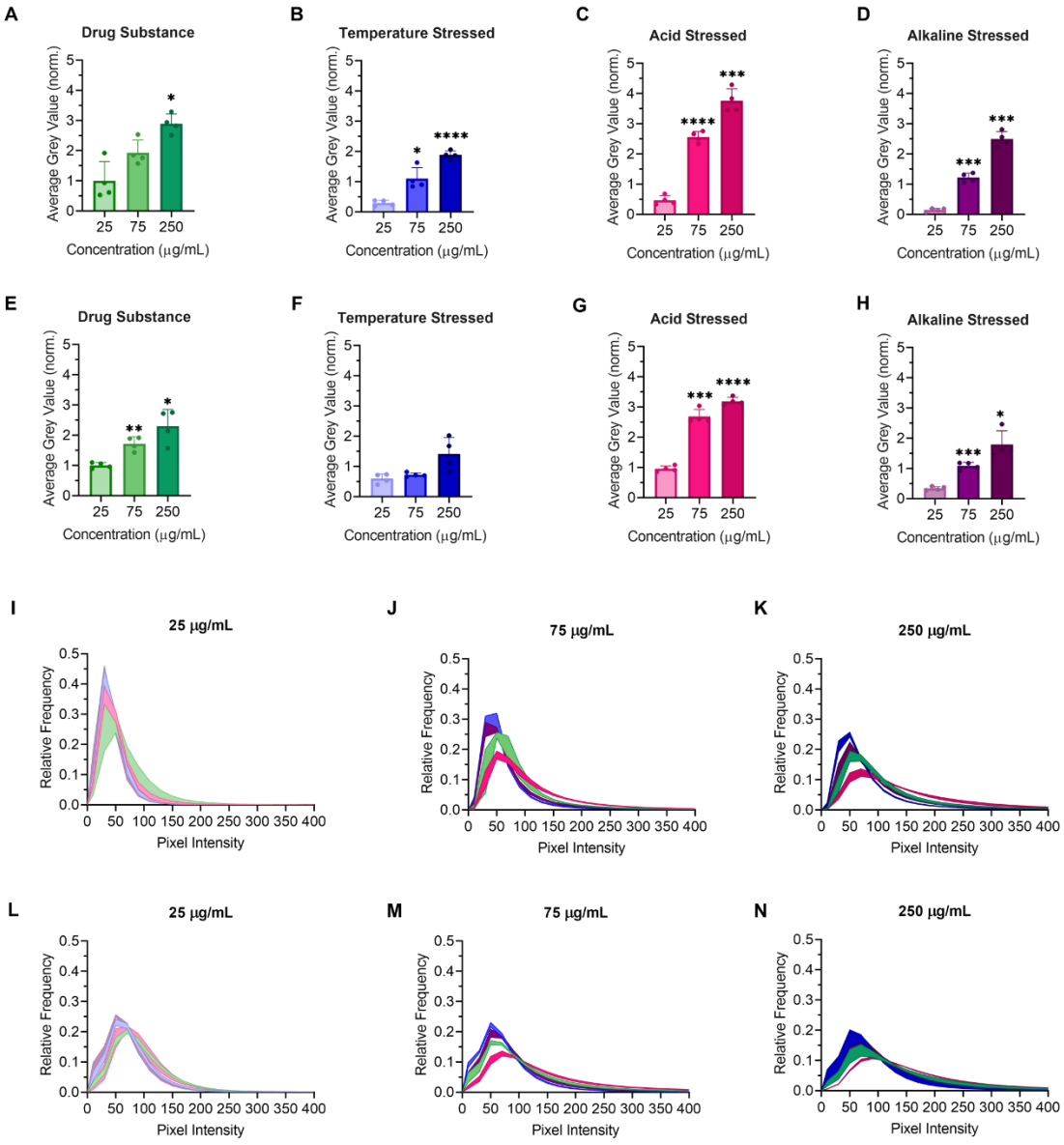

Figure S6. Lubricin adsorbed on StcE-treated hTCEpi and HCjE cells in a dose-dependent manner. **(A-H)** Lubricin adsorbed on both StcE-treated **(A-D)** hTCEpi and **(E-H)** HCjE cells in a dose-dependent manner, but the adsorbed amount of recombinant lubricin **(A, E)** or lubricin subjected to temperature stress **(B, F)**, acid stress **(C, G)**, and alkaline stress **(D, H)** varied based on incubation conditions. Statistical significance ($p < 0.05$) was determined using one-way Welch ANOVA with post-hoc Dunnett's T3 multiple comparisons testing relative to 25 µg/mL supplementation. Lubricin adsorption behavior (data: mean ± S.D. error envelope, n = 4) on StcE-treated **(I-K)** hTCEpi and **(L-N)** HCjE cells differed, with fewer adsorption differences

observed between variants on HCjE cells and reduced differences observed between variants on hTCEpi cells as solution concentration increased.

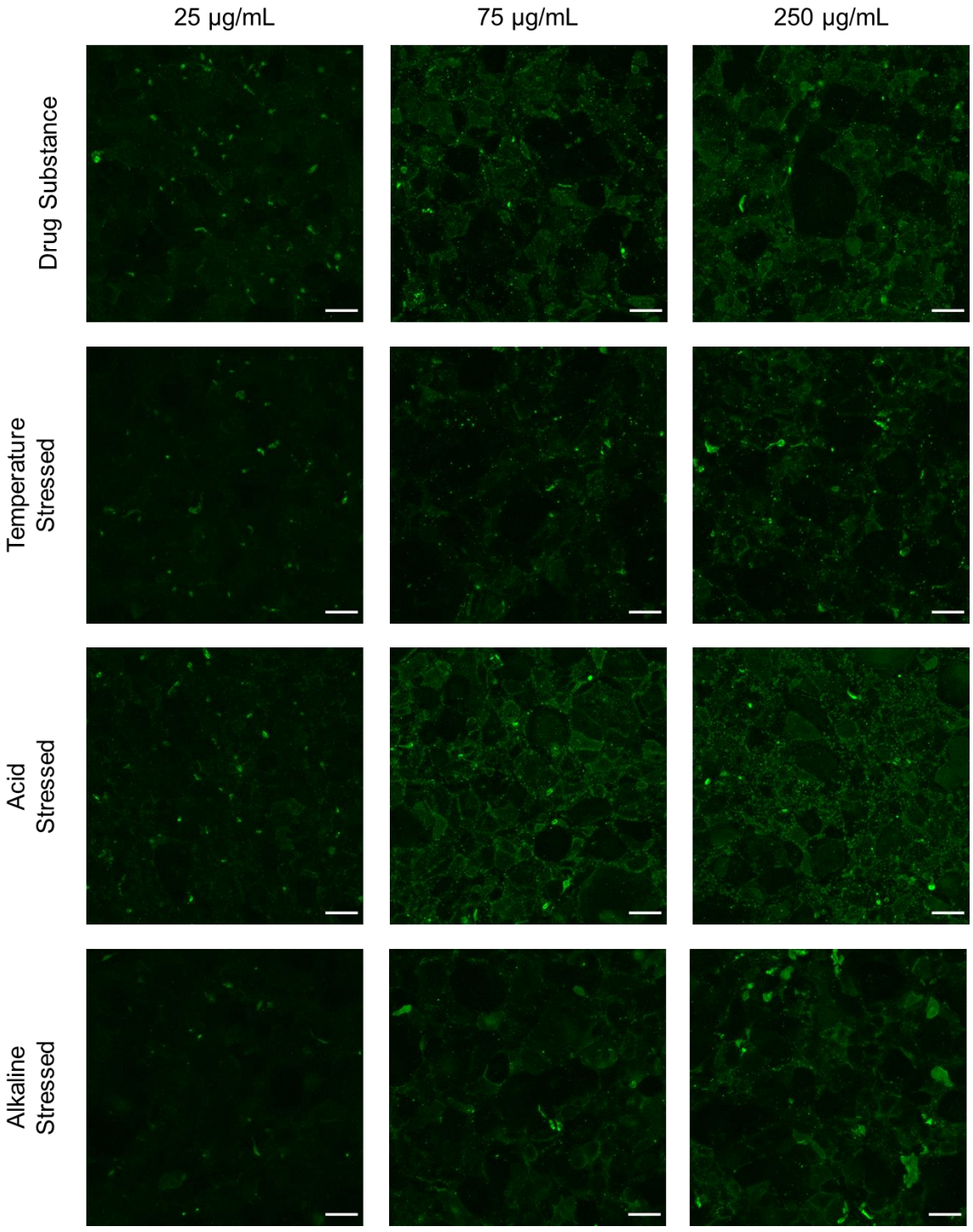

Figure S7. Recombinant human lubricin and lubricin subjected to accelerated aging conditions adsorbed to StcE-treated differentiated HCjE cells in a dose-dependent manner (scale bar: 100 µm).

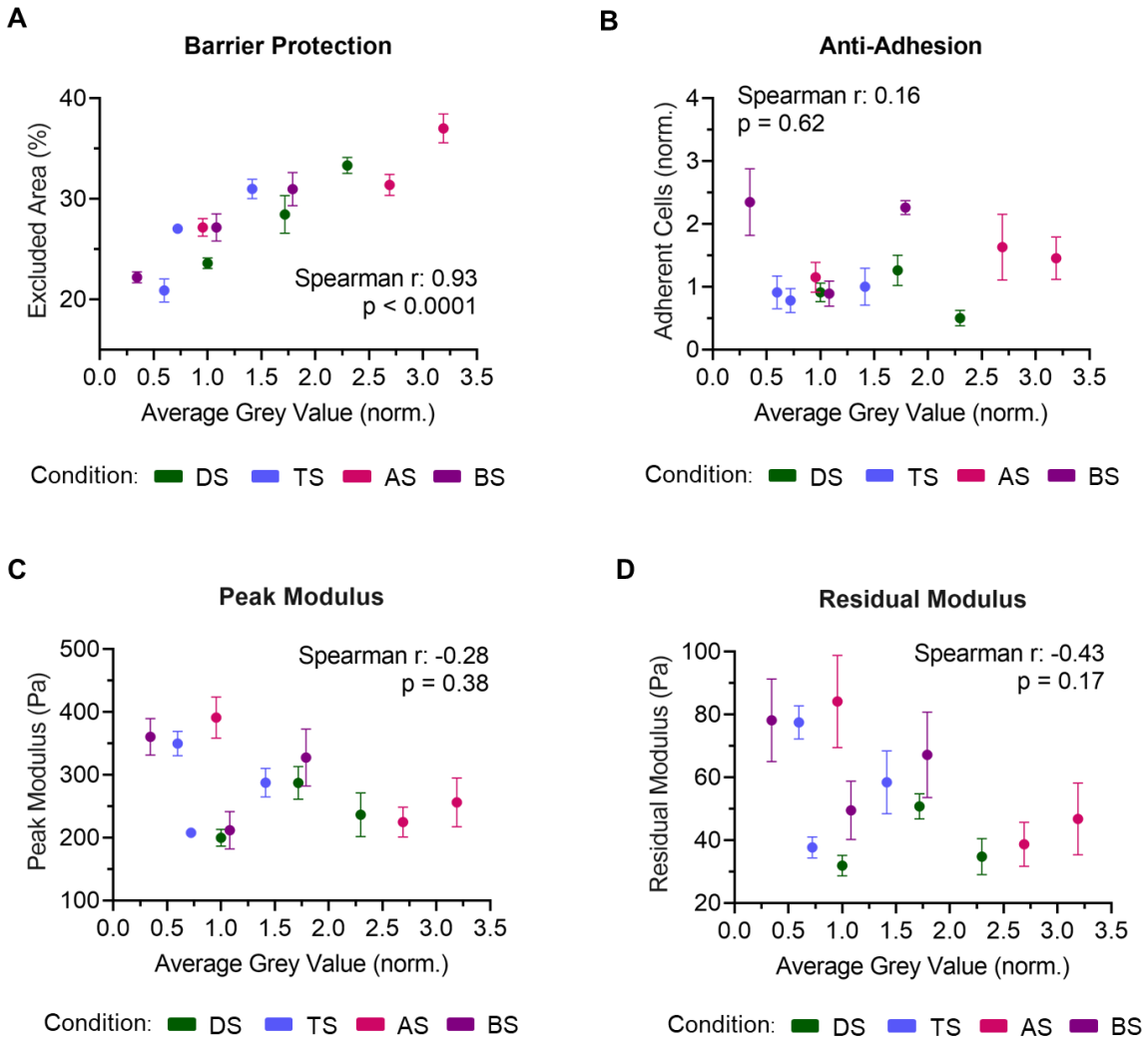

Figure S8. Lubricin bioactivity is not directly correlated with unstressed and aged lubricin surface coverage. While rose-bengal dye exclusion (data = mean ± S.E., n = 4) **(A)** was tightly correlated with lubricin surface coverage, **(B)** anti-adhesion behavior on StcE-treated hTCEpi cells (data = mean ± S.E., n = 4) and **(C, D)** biolubrication (data = mean ± S.E., n = 7-12) properties exhibited weak correlations with surface coverage.